INSTITUTE FOR FUSION STUDIES

DOE/ET-53088-500 IFSR #500

Impurity and Neutral Effects
on the Dissipative Drift Wave
in Tokamak Edge Plasmas

Y.Z. ZHANG AND S.M. MAHAJAN
Institute for Fusion Studies
The University of Texas at Austin
Austin, Texas 78712

May 1991

THE UNIVERSITY OF TEXAS

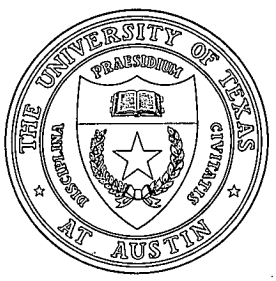

AUSTIN

List of Changes for the revised version

1. Page 5.

Change: " $< L_n$, the already defined scale length for the ambient plasma " to " is not too large " in line 14.

Delete: " magnified by a factor $L_n/L_z > 1$, resulting in " in line 18.

Change: " L_n/L_z " to " L_z " in line 19.

2. Page 7, Eq.(9).

Delete the last term of the Eq.(9).

3. Page 12.

Delete: " and $L_n/L_z > 1$, " in line 16.

Add: " if $|L_z|$ is not too large, e.g. not larger than the minimum of the density and the temperature gradient lengths, " in line 17.

4. Page 15. a big change [cf. the attached sheet]

5. Page 23.

Change " sharper than the density gradients of the plasma " to " reasonably sharp " in line 20.

Add: " Note that the relavant parameter for the drive is the scale length L_z associated with the impurity density; the appearance of L_n/L_z in various equations is an artifact of our normalization. In fact, the combination $\omega^*_{en} L_n$ that appears in the impurity response is independent of L_n. " in line 21.

are neglected. For very small value of Υ [weakly collisional plasma, regime (a), $\Upsilon = 0.04$] a narrow current channel near the rational surface results in a very shallow potential well unable to contain the mode, which is primarily localized by the ion sound effect [Fig. 1*a*]. The situation illustrated in Fig. 1*b* is quite different. Here $\Upsilon = 0.18$ has a moderate value, and the current channel created potential value is deep enough to localize the mode; the ion sound term plays no essential role. As Υ is increased further [Fig. 1*c*, $\Upsilon = 0.6$] the current channel width increases towards $x = x_s$, and the structure of the mode becomes sensitive to the ion sound term. Finally, when $\Upsilon = 1$, the current channel, though broad, becomes sufficiently shallow that the mode structure is again controlled by the sound term [Fig. 1*d*]. Strictly speaking, our set of equations is inadequate to accurately describe the last scenario.

We now examine the comparative roles of the destabilizing mechanisms for standard edge plasma condition in TEXT. The parameters chosen for numerical work are: $R = 100\,\mathrm{cm}$, $a = 25\,\mathrm{cm}$, $n_e = 3 \times 10^{12}\,\mathrm{cm}^{-3}$, $T_e = 20\,\mathrm{ev}$, $B = 22\,\mathrm{kG}$, $L_n = 5\,\mathrm{cm}$, $L_z = 1\,\mathrm{cm}$, $L_s = 150\,\mathrm{cm}$, $Z = 4$, V_{loop} (the loop voltage)=1 Volt, $\tau_i = 1.0$, $\eta_e = 1.0$, $\eta_i = 0.5$, and the poloidal mode number $m = 30$. [For the electron temperature $\sim 20\,\mathrm{ev}$, the impurity charge number is $Z \sim 4$]. We do not include the effect from $\nu_z'(\sim \partial I_z/\partial T_e)$, because the strong temperature dependence of $I_z(T_e)$ for a given charge state of a given impurity will be smeared out by averaging over many impurity species and multiple charge states of the same impurity. The value of $n_z I_z(T_e)$ is estimated from the experimental data (notice that only the product of n_z and $I_z(T_e)$ is the relevant parameter for the impurity condensation drive). From the Bolometry measurement on TEXT,[19,20] we choose the radiation power loss rate as 0.06 Watt/cm^3, which, for standard value of n_e, translates to $n_z I_z(T_e) = 2 \times 10^{-7}\,\mathrm{erg/s}$. All standard parameters are followed by the symbol (1), for example, the standard ν_{ei}, and ω_{en}^* are written as $\nu_{ei}(1) = 1.26 \times 10^6/\mathrm{s}$, $\omega_{en}^*(1) = 2.18 \times 10^4/\mathrm{s}$ respectively. From the above standard data, we obtain $\overline{\beta}_\nu(1) = 0.35$, $\widehat{\nu}_z(1) = 0.2$, $k^2(1) = 0.04$, $\overline{J}_\parallel(1) = 0.1$.

By varying the value of the equilibrium current and collisionality, we can examine the

Impurity and Neutral Effects on the Dissipative Drift Wave in Tokamak Edge Plasmas

Y.Z. Zhang and S.M. Mahajan
Institute for Fusion Studies
The University of Texas at Austin
Austin, Texas 78712

Abstract

Possible destabilizing mechanisms for the linear electrostatic dissipative drift waves (in tokamak edge plasmas) are investigated in slab geometry. The effects of processes such as ionization, charge exchange, radiation, and rippling are examined. In particular, the impurity condensation associated with radiation cooling is evaluated appropriately for the drift wave ordering, which is found to be an important driving mechanism in contrast to the results of earlier studies.[1] It is also shown that the role of ionization is quite complicated, and depends strongly on the manner in which the equilibrium is achieved. The linear eigenmode equation is studied both analytically and numerically. For the range of parameters relevant to TEXT tokamak, both the charge exchange and the rippling effect are found to be unimportant for instability.

I. Introduction

The highly diagnosed edge region of a tokamak plasma provides a valuable testing ground for turbulence theories. The motivation to theoretically investigate this region has become even stronger with the discovery of the H-mode,[2] a state of the plasma characterized by improved confinement. It is observed that the H-mode is often accompanied by a suppression in the level of edge turbulence.[3,4] This correlation suggests that a deeper understanding of edge turbulence could help in creating and sustaining this highly desirable plasma equilibrium.

Several reasonable models for the suppression of edge turbulence have been recently advanced and have met with a certain degree of success.[5–7] Strangely enough, the causes and nature of the original edge turbulence (supposedly suppressed by the proposed mechanisms) are still essentially ununderstood.[1] In several of the current theories, the edge turbulence is attributed to rippling — like modes, which are assumed to have no perturbed pressure ($\delta P_e = 0$).[8,9] This assumption runs into several difficulties. Zero perturbed pressure implies that the perturbed temperature (δT_e) should be strongly correlated with the perturbed density (δn). Experiments on the TEXT tokamak, however, reveals that $\delta n - \delta T_e$ is the weakest amongst $\delta n - \delta T_e, \delta n - \delta\varphi$ and $\delta\varphi - \delta T_e$ correlations, the last being the strongest.[10] (It shoud be pointed out that the electrostatic potential $\delta\varphi$ measured by the Langmuir probe in TEXT is the floating, rather than the plasma potential). From a theoretical point of view, the zero pressure fluctuation is essentially a strong assumption on the parallel Ohm's law, which is plausible if the mode localization is shifted sufficiently away from the rational surface, i.e., it is restricted only to the strong rippling case, whereof just a small overlap occurs between the perturbed current $\delta J_{||}$ (localized at the rational surface) and other shifted fluctuations such as $\delta\varphi, \delta n, \delta T_e$. However, the strong rippling regime requires a large equilibrium current, a condition generally not satisfied for the typical edge plasmas (cf. Sec. IV for detail). To model the realistic situation, therefore, it is essential that the

self-consistent pressure fluctuations be included in deriving the mode equations, even if the parallel fluid motion is decoupled from the system because the ion sound effects are ignorable. The preceding discussion strongly suggests that the identification of the linear mode responsible for edge turbulence is still not complete.

Since the edge plasma is highly collisional, Braginskii transport equations[11] can be used to model the plasma dynamics. In a slab geometry, this model can adequately describe the dissipative drift wave. Recent numerical simulation of the dissipative drift wave turbulence reveals several features that appear to be consistent with experiment.[12] For example, the $\delta T_e - \delta\varphi$ correlation is found to be stronger than the $\delta n - \delta\varphi$ correlation. The linear aspects of the dissipative drift wave for a pure plasma have been studied by Drake and Hassam,[13-14] and Chen *et al.*[15]

In the limit of small ion Larmor radius, the nature of the mode is controlled by the parameter $\Upsilon = x_r/x_s = (2\omega\nu_e/k_{\|}'^2 v_e^2)^{1/2}(\omega/c_s k_{\|}')^{-1} = [(m_e/m_i)(\nu_e/\omega)]^{1/2}$, the ratio of the current channel width to the ion-sound-point distance from the rational surface. In the above definition, $\omega(< \nu_e)$ is the mode (electron collision) frequency, $k_{\|}' \equiv k_y/L_s$ [$k_y \equiv m/r$, $L_s = qR/\hat{s}$], m is the poloidal mode number, r (R) is the minor (major) radius, q is the safety factor, $v_e = (2T_e/m_e)^{1/2}$ is the electron thermal velocity, $c_s^2 = T_e/m_i$ is the ion sound speed, $\hat{s} \equiv (r/q)(dq/dr)$ is the magnetic shear parameter, T_e is the electron temperature, and m_e (m_i) is electron (ion) mass. For generic drift waves, the parameter $\Upsilon = [(m_e/m_i)(\nu_e/\omega_{en}^*)]^{1/2}$, because the mode frequency $\omega \sim \omega_{en}^* \equiv T_e c k_y/eBL_n$, where c is the speed of light, e is the electron charge ($e > 0$), B is the magnetic field, and $L_n = (-dln\ n/dx)^{-1}$ is the density gradient scale length. Three distinct regimes pertain: (a) The weakly collisional regime $\Upsilon \ll 1$, in which the mode localization (in close analogy with the collisionless drift waves) is provided by the ion sound term. (b) The collisional regime, where $\Upsilon < 1$ but neither too small nor close to unity. The current channel is now broad enough to produce a localizing potential well. The mode width is determined by x_r, and the ion sound effects are

unimportant. This is the regime most relevant to existing tokamak edge plasmas. (c) The strongly collisional regime characterized by Υ close to or even greater than unity, in which the current channel expands to overlap with the ion sound region. The current channel potential becomes shallow (high collisionality prohibits parallel heat flow) and the ion sound effect are essential for the mode localization. This regime may also be relevant to some edge plasma. A proper treatment of the highly collisional regime [regime (c)] would require a very complicated set of equations, because in this regime the electron-ion energy transfer time is comparable to the wave period. In the present paper, therefore, we confine ourselves to regime (b) $\Upsilon < 1$. In the rest of the paper, unless stated otherwise, the 'dissipative drift wave' will refer to regime (b) only.

For typical edge plasma parameters in TEXT the dissipative drift wave is linearly stable in a pure electron and ion plasma. To investigate possible sources of instability we generalize the previous studied system[13–15] to a multispecies plasma, including neutrals and impurities. The interaction of new components with the bulk species, electron and ions, provide extra dissipations that may drive the mode unstable. The basic linear system primarily using equations derived by Braginskii with simplifying approximations warranted by experimental scenario are given in Sec. II.

At tokamak edge, the neutral density is typically one to several per cent of the electron density. Through the processes of ionization and charge exchange, the neutrals change the plasma dynamics by introducing a source term in the continuity equation, and a frictional force in the charged fluid momentum transfer equation. A general analysis for the neutral responses is complicated, and will not be presented in this paper. The analysis can be greatly simplified, if the neutral temperature is not too much lower than the bulk plasma temperature (the warm neutral limit), in which case the neutral fluid can be viewed as imcompressible. The role of charge exchange is associated with the ion sound effect, which is unimportant for the dissipative drift wave. Even in the warm neutral limit, however, the

role of ionization is very complicated, and strongly depends on the manner in which the equilibrium is achieved. For this reason the issue of ionization is discussed seperately in Sec. VI, and will not be included in the eigenmode analysis.

The importance of impurities for the edge plasma has been appreciated for a long time. It contributes to both the rippling effect[16,8,9,17] and the radiation cooling.[18,8,1] Previous calculations, limited to a purely growing mode,[16] neglected the impurity inertia. This response can not be appropriate for the dissipative drift wave in the presence of massive impurities, because the inertial term gets enhanced due to comparatively high mode frequency $\omega \sim \omega_{en}^{*}$. In fact, the inertial term (proportional to ω) could be dominant in the impurity response to a drift wave, because the impurity sound speed c_{sz}, [where $c_{sz}^2 = T_z/m_z$ with T_z the impurity temperature $\leq T_i$, the bulk ion temperature, and m_z the impurity mass $\gg m_i$], is much smaller than the bulk ion sound speed c_s. It turns out that if the the impurity gradients are stronger than the bulk plasma gradients, i.e., if $L_z = (dln\ n_z/dx)^{-1}$ [n_z the impurity density] $< L_n$, the already defined scale length for the ambient plasma, the impurity density response is greatly simplified, and becomes a term proportional to $\delta\varphi$. When this newly calculated response is used for the impurity condensation effect on radiation cooling power in the electron temperature evolution equation, it is found that the dissipation due to radiation is magnified by a factor $L_n/L_z > 1$, resulting in an important driving force for the dissipative drift wave (positive L_n/L_z is destabilizing). A detailed derivation for the neutral and impurity responses is given in Sec. III.

The remaining part of this paper is organized as follows. In Sec. IV the linear eigenmode equation is derived, and solved numerically, analyzing and comparing the relative importance of various driving forces. Some of numerical results are presented in a manner that makes comparison with experiment easier. In Sec. V, the simplified eigenmode equation is solved analytically by the WKB method, neglecting both the rippling, and the ion sound effects. A brief summary of the paper along with our conclusions is the subject of Sec. VII.

II. Basic Equations, Linearization

Our theoretical model is based on Braginskii transport equations. Unless stated otherwise, the analysis is confined to electrostatic mode in slab geometry. The system consists of hydrogenic ions and neutrals, and only one impurity species in a uniform equilibrium electric field. Since we are concentrating on delineating the growth mechanism, the gradients of the radial electric field are neglected.In the presence of neutrals the electron continuity equation becomes

$$\frac{\partial n_e}{\partial t} + \nabla \cdot (n_e \mathbf{v}_e) = \nu_I n_e \ , \tag{1}$$

where n_e is the electron density, $\nu_I = f_I(T_e) n_0$, is the ionization rate due to electron impact, n_0 is the neutral density, and $f_I(T_e)$ is a function weakly dependent on the electron temperature. The electron fluid velocity $\mathbf{v}_e = v_{e,\|}\mathbf{b} + \mathbf{v}_{e,\perp}$, ($\mathbf{b}$ is the unit vector along the equilibrium magnetic field) has the parallel component $v_{e,\|}$, and the perpendicular component

$$\mathbf{v}_{e,\perp} = \frac{c}{B}\mathbf{b} \times (\nabla\varphi - \frac{1}{en_e}\nabla P_e) \ , \tag{2}$$

which consists of $\mathbf{E} \times \mathbf{B}$ and diamagnetic drift with φ the electrostatic potential, and $P_e = n_e T_e$, the electron pressure. The equation of parallel electron momentum balance is generally replaced by the equivalent Ohm's law

$$\eta J_\| = E_\|^{(0)} - \nabla_\| \varphi + \frac{1}{en_e}\nabla_\| P_e \ , \tag{3}$$

where $E_\|^{(0)}$ is the equilibrium parallel electric field, $J_\|$ is the electric current, $\nabla_\| \equiv \mathbf{b} \cdot \nabla$, and η is the resistivity. With impurities, we write $\eta = Z_{\text{eff}}\eta_{sp}$, where $Z_{\text{eff}} \equiv 1 + Z^2 n_z/n_e$, with n_z the impurity density, Z the impurity charge number, and $\eta_{sp}(\equiv m_e\nu_{ei}/e^2 n_e)$ the Spitzer resistivity. The electrostatic potential $\delta\varphi$ and the parallel current $J_\|$ are coupled through the vorticity equation

$$m_i n_i \left(\frac{c}{B}\right)^2 \left(\frac{d}{dt}\right)_i \nabla_\perp^2 \varphi = \nabla_\| J_\| \ , \tag{4}$$

where $(d/dt)_i \equiv \partial/\partial t + (\mathbf{u}_E + \mathbf{u}_{D_i}) \cdot \nabla$, $\mathbf{u}_E = (c/B)\mathbf{b} \times \nabla\varphi$ is the $E \times B$ drift velocity, $\mathbf{u}_{D_i} = (c/Ben_i)\mathbf{b} \times \nabla P_i$ is the ion diamagnetic velocity, and $P_i = n_i T_i$, is the ion pressure. In Eq. (4) we have neglected the impurity contribution to the fluid inertia for simplicity; this contribution yields a small quantitative stabilizing effect on the system. With charged impurities in the system, it is useful to write the parallel momentum equation for the total charged fluid,

$$m_i n_i \left(\frac{d}{dt}\right)_E u_{i,||} + m_z n_z \left(\frac{d}{dt}\right)_E u_{z,||} + \nabla_{||}(P_e + P_i + P_z) = \nu_x m_i n_i (u_{0,||} - u_{i,||}) + \nu_I m_0 n_e u_{0,||} \ , \quad (5)$$

where $(d/dt)_E \equiv \partial/\partial t + \mathbf{u}_E \cdot \nabla$; $u_{i,||}, u_{z,||}$ and $u_{0,||}$ are representing the parallel ion, impurity and neutral velocities. $\nu_x = f_{ex}(T) n_0$ is the charge exchange rate, and $P_z = n_z T_z$ is the impurity pressure. Since ion temperature evolution is neglected in our study, we need only the electron temperature equation

$$\left(\frac{\partial}{\partial t} + \mathbf{u}_E \cdot \nabla - \beta_\nu \nabla_{||}^2\right) T_e = H - L - T_e \nabla_{||} v_{e,||} \ , \quad (6)$$

to complete our description of the bulk plasma. In Eq. (6) $\beta_\nu \equiv T_e/e^2 n_e \eta$ describes the parallel heat conduction, H is the heating source, and $L = (2/3) n_z I_z(T_e)$ with I_z the radiation cooling function, describes the impurity radiation loss.

To close our system we also need equations associated with neutral and impurity component. These are the neutral and impurity continuity equations

$$\frac{\partial n_0}{\partial t} + \nabla \cdot (n_0 \mathbf{u}_0) = -\nu_I n_e \ , \quad (7)$$

$$\frac{\partial n_z}{\partial t} + \nabla \cdot (n_z \mathbf{u}_z) = 0 \ , \quad (8)$$

where $\mathbf{u}_0$ ($\mathbf{u}_z$) is the neutral (impurity) velocity, with the impurity perpendicular velocity given by

$$\mathbf{u}_{z,\perp} = \frac{c}{B}\mathbf{b} \times (\nabla\varphi + \frac{1}{Zen_z}\nabla P_z) - \frac{m_z}{Ze}\left(\frac{c}{B}\right)^2 \left(\frac{d}{dt}\right)_z \nabla_\perp \varphi \ , \quad (9)$$

with $[(d/dt)_z \equiv (d/dt)_{i\to z}]$, the neutral momentum equation

$$m_i n_0 \frac{d}{dt}\mathbf{u}_0 + \nabla P_0 = \nu_x m_i n_i(\mathbf{u}_i - \mathbf{u}_0) - \nu_I m_i n_e \mathbf{u}_0 \ , \tag{10}$$

where $P_0 = n_0 T_0$, and $d/dt \equiv \partial/\partial t + \mathbf{u}_0 \cdot \nabla$, and the impurity parallel momentum equation

$$m_z n_z \left(\frac{d}{dt}\right)_E u_{z,\|} + \nabla_\| P_z = Z e n_z E_\| + n_i m_i \nu_{iz}(u_{i,\|} - u_{z,\|}) + n_e m_e \nu_{ez}(v_{e,\|} - u_{z,\|}) \ , \tag{11}$$

where $\nu_{iz}(\nu_{ez})$ is the ion-impurity (electron-impurity) collision frequency.

In the above theoretical model all equilibrium quantities are assumed to vary only in the radial direction, in particular quantities like $\nabla_\| T_e^{(0)} = \nabla_\| n_e^{(0)} = 0$, where the superscript (0) denotes equilibrium. We also assume that $\delta T_z, = \delta T_i = \delta T_0 = 0$, i.e., the temperature fluctuations for ions, impurities and neutrals are negligible. This asuumption is plausible if Υ is sufficiently smaller than unity that the electron-ion energy transfer time is much longer than the wave period. To simplify our discussion we also assume that $u_{i,\|}^{(0)} = u_{0,\|}^{(0)} = u_{z,\|}^{(0)} = 0$. Notice that the already invoked electrostatic approximation requires that $\omega/\nu_{ei} \ll (ck_\perp/\omega_{pe})^2$, where $\omega_{pe}^2 \equiv 4\pi n_e e^2/m_e$ with $k_\perp$ the perpendicular wave number. This condition is generally satisfied for typical edge plasmas in TEXT.

Before linearizing Eqs.(1)-(11) for stability analysis, we have to discuss a particular serious problem associated with the inclusion of ionization. In slab geometry, wherein all equilibrium quantities are assumed to vary only in the radial direction, the divergence of the equilibrium current (when Eq. (2) is employed), $\nabla \cdot (n_e^{(0)}\mathbf{v}_e^{(0)}) = (c/B)\mathbf{b} \cdot \nabla\varphi^{(0)} \times \nabla n^{(0)} = 0$ leading to (through Eq. (1))

$$\frac{\partial}{\partial t} ln\ n_e^{(0)} = \nu_I^{(0)} \ . \tag{12}$$

with the implication that with $\nu_I^{(0)} \neq 0$, there is no equilibrium ($\partial/\partial t = 0$) electron density. In order to include a possible slow time variation of $n_e^{(0)}$, the linearized version of the continuity equation is then written in a general form

$$\frac{\partial}{\partial t}\frac{\delta n_e}{n_e^{(0)}} + \nabla \cdot \delta\mathbf{v}_e + \delta\mathbf{v}_e \cdot \nabla ln\ n_e^{(0)} + \mathbf{v}_e^{(0)} \cdot \nabla \frac{\delta n_e}{n_e^{(0)}} = \delta\nu_I \ , \tag{13}$$

where $\delta\nu_I = \nu_I^{(0)}\delta n_0/n_0^{(0)} + (\partial\nu_I/\partial T_e)^{(0)}\delta T_e$. The remaining linear equations can be obtained in a straightforward manner with the understanding that the density may grow slowly, while other quantities like temperature and current are genuine equilibrium quantities. The set of linearized equations consist of: parallel Ohm's law

$$\delta\eta J_{\|}^{(0)} + \eta^{(0)}\delta J_{\|} = -\nabla_{\|}\delta\varphi + \frac{1}{e}\nabla_{\|}\delta T_e + \frac{T_e^{(0)}}{e}\nabla_{\|}\frac{\delta n_e}{n_e^{(0)}} \tag{14}$$

with $\delta\eta = \delta Z_{\rm eff}\eta_{sp}^{(0)} + Z_{\rm eff}^{(0)}\delta\eta_{sp}$; the vorticity equation [Eq. (4)]

$$m_i n_i^{(0)}\left(\frac{c}{B}\right)^2\left(\frac{d}{dt}\right)_i^{(0)}\nabla_{\perp}^2\delta\varphi = \nabla_{\|}\delta J_{\|}\ , \tag{15}$$

where $(d/dt)_i^{(0)} \equiv \partial/\partial t + (\mathbf{u}_E^{(0)} + \mathbf{u}_{D_i}^{(0)})\cdot\nabla$ with $\mathbf{u}_E^{(0)} = (c/B)\mathbf{b}\times\nabla\varphi^{(0)}, \mathbf{u}_{D_i}^{(0)} = (c/Ben_i^{(0)})\mathbf{b}\times\nabla P_i^{(0)}$; the parallel momentum equation [Eq. (5)]

$$\left(\frac{d}{dt}\right)_E^{(0)}\delta u_{i,\|} + \frac{m_z n_z^{(0)}}{m_i n_e^{(0)}}\left(\frac{d}{dt}\right)_E^{(0)}\delta u_{z,\|} + (1+\tau_i)c_s^2\nabla_{\|}\left(\frac{\delta n_e}{n_e^{(0)}}\right) + \frac{1}{m_i}\nabla_{\|}\delta T_e$$
$$= \nu_x(\delta u_{0,\|l} - \delta u_{i,\|}) + \nu_I\delta u_{0,\|}\ , \tag{16}$$

where $(d/dt)_E^{(0)} \equiv \partial/\partial t + \mathbf{u}_E^{(0)}\cdot\nabla$, with $\nabla_{\|}\delta P_z$ neglected, and the equation for electron temperature evolution

$$\left(\frac{\partial}{\partial t} + \mathbf{u}_E^{(0)}\cdot\nabla - \beta_\nu\nabla_{\|}^2\right)\delta T_e + \delta\mathbf{u}_E\cdot\nabla T_e^{(0)} = -\frac{2}{3}\delta n_z I_z^{(0)} - \frac{2}{3}n_z^{(0)}\cdot\frac{\partial I_z^{(0)}}{\partial T_e}\delta T_e - T_e^{(0)}\nabla_{\|}\delta v_{e,\|}\ , \tag{17}$$

where $\delta\mathbf{u}_E = (c/B)\mathbf{b}\times\nabla\delta\varphi$. Although the fluctuating part of H may be quantitatively important, it is being neglected for simplicity.

The linearized form for neutral and impurity equation [Eqs. (7)–(11)] will be derived in the next section.

III. The Neutral and Impurity Responses

We first show that for warm neutrals ($T_0 \sim T_i$) the neutral density does not respond to the drift wave with a large perpendicular wave number $k_\perp$. For notational simplicity, the superscript (0) for the equilibrium quantities will be dropped except in Sec. VI.

To calculate the neutral response, we linearize Eq. (7) and Eq. (10) to obtain

$$\left(\frac{\partial}{\partial t}+\mathbf{u}_0\cdot\nabla\right)\left(\frac{\delta n_0}{n_0}\right)=-(\nu_I\frac{n_e}{n_0})\cdot\frac{\delta n_e}{n_e}-\delta\mathbf{u}_0\cdot\nabla ln\ n_0-\nabla\cdot\delta\mathbf{u}_0\ . \tag{18}$$

and

$$m_0n_0\left(\frac{\partial}{\partial t}+\mathbf{u}_0\cdot\nabla\right)\delta\mathbf{u}_0+\nabla T_0\delta n_0=\nu_x m_i n_i(\delta\mathbf{u}_i-\delta\mathbf{u}_0)-\nu_I m_0 n_e\delta\mathbf{u}_0$$
$$-\nu_x m_i\mathbf{u}_{i,\perp}\delta n_i-(\nu_x+\nu_I)m_i\mathbf{u}_0\delta n_e\ . \tag{19}$$

The equlibrium neutral velocity $\mathbf{u}_0$, can be driven radially by the neutral pressure gradient, and poloidally by the bulk ions through charge exchange. Because the details for the neutral equilibrium solution are not essential to the following discussion [actually, these are not trivial], we merely give an estimate for $\mathbf{u}_0$. The radial (x) component of $\mathbf{u}_0$ is estimated as $g(x)c_{so}(\nu_I/\nu_x)^{1/2}$, where $g(x)$ may vary from order unity to a small number, and c_{so} is the neutral sound speed [$c_{so}\equiv(T_0/m_0)^{1/2}>10^6$cm/s for $T_0>1ev$]. Notice that in an equilibrium the radial component of $\mathbf{u}_0$ can not be zero with finite ν_I. The poloidal component of $\mathbf{u}_0$ (in y-direction) is estimated as $u_{i,y}$, the poloidal bulk ion velocity, whereas $u_{0,||}=0$, because there is no parallel driving force on the neutrals ($u_{i,||}=0$). In the warm neutral limit one may order $\omega/c_{so}k_\perp,(\nu_x n_e/n_0)/c_{so}k_\perp,(\nu_I n_e/n_0)/c_{so}k_\perp\sim\epsilon\ll 1$, leading to [through Eq. (19)] the following estimates $\delta\mathbf{u}_{0,\perp}\sim c_{so}(\delta n_0/n_0)$ for $g(x)\sim O(1)$, and $\delta\mathbf{u}_{0,\perp}\sim(c_{so}/\epsilon)(\delta n_0/n_0)$ for $g(x)\ll 1$. For the former case ($g(x)\sim O(1)$) the perpendicular compressional term in Eq. (18) is compaprable to the convective term, which yields $\delta n_0/n_0\sim\epsilon\delta n_e/n_e$. For the later case ($g(x)\ll 1$) the perpendicular compressional term becomes dominant, and we find $\delta n_0/n_0\sim\epsilon^2\delta n_e/n_e$. In either case, the warm neutral fluid can be viewed as incompressible, $\delta n_0/n_0$ can be dropped everywhere. The demonstrated incompressibility of neutral would, by itself, lead to considerable simplification. However, in this paper, we make even a stronger assumption: we neglect the effects of ionization altogether ($\nu_I=0$) because a consistent incorporation of ionization needs more analysis [Sec. VI].

If $g(x) \sim O(1)$, the parallel component of Eq. (19) yields $\delta u_{0,\|} \sim \epsilon \delta u_{i,\|}$. The contribution from neutrals to the parallel momentum equation [Eq. (16)] can thus be neglected. For $g(x) \ll 1, \delta u_{0,\|}$ is comparable to $\delta u_{i,\|}$, and is given by $[g(x) \to 0]$

$$\delta u_{0,\|} = \frac{i\nu_x}{\omega + i\nu_x(n_i/n_0)} \cdot \frac{n_i}{n_0} \delta u_{i,\|} \ . \tag{20}$$

Substituing Eq. (20) into Eq. (16), we find the ion parallel response modified by the neutrals,

$$\delta u_{i,\|} = \frac{1}{\Omega_x} \left\{ -\frac{m_z n_z}{m_i n_i} \omega' \delta u_{z,\|} + (1+\tau_i) c_s^2 k_\| \frac{\delta n_e}{n_e} + \frac{k_\|}{m_i} \delta T_e \right\} \ , \tag{21}$$

where $\Omega_x \equiv \omega' + i\nu_x \omega'/(\omega + i\nu_x n_i/n_0)$, $\omega' = \omega - \omega_E, \omega_E \equiv u_E k_y$ is the $\mathbf{E} \times \mathbf{B}$ rotation frequency due to equilibrium electric field, and $\tau_i \equiv T_i/T_e$. It is interesting to note that in the large ν_x limit Ω_x goes to $(1 + n_0/n_i)\omega' \sim \omega'$, indicating that the charge exchange is unlikely to be an important driving force for this system. Henceforth, we approximate Ω_x by ω', and drop the superscript on ω, i.e., ω denotes the mode frequency in the plasma frame, or equivalently, $(d/dt)_E \to \partial/\partial t$.

Now, we calculate the impurity response to the dissipative drift wave. The linearized impurity continuity equation [Eq. (8)] is

$$\frac{\partial}{\partial t} \delta n_z + n_z \left[\nabla_\| \delta u_{z,\|} - i\omega_{en}^* \frac{L_n}{L_z} \delta\hat{\varphi} \right] = 0 \ , \tag{22}$$

where $\delta\hat{\varphi} \equiv e\delta\varphi/T_e$, and where we have neglected the contribution from impurity polarization current. In order to calculate $\delta u_{z,\|}$, we must solve the linearized impurity parallel momentum equation [Eq. (11)],

$$m_z n_z \frac{\partial}{\partial t} \delta u_{z,\|} + \nabla_\| \delta P_z = Ze E_\| \delta n_z - Z e n_z \nabla_\| \delta\varphi + \delta F_{z,\|} \ , \tag{23}$$

where $\delta F_{z,\|}$ represents the linear frictional forces on the impurity fluid due to electrons and ions, i.e.,

$$F_{z,\|} \equiv n_i m_i \nu_{iz} (\delta u_{i,\|} - \delta u_{z,\|}) + n_e m_e \nu_{ez} (v_{e,\|} - \delta u_{z,\|}) \ , \tag{24}$$

where ν_{ez} is taken as $(Z_{\rm eff}Zn_z/n_e)\nu_{ei}$, so that the equilibrium condition of Eq. (11) is consistent with our assumption $u_{i,\|} = u_{z,\|} = 0$. The definition for the total parallel current: $J_\| = en_i\delta u_{i,\|} + Zen_z\delta u_{z,\|} - en_e v_{e,\|}$, and the estimate $\nu_{ez}/\nu_{iz} \sim (m_i/m_e)^{1/2}$ helps convert the second term on the r.h.s. of Eq. (24) to $-(m_e/e)\nu_{ez}J_\|$. Making use of this estimate along with the parallel Ohm's law [Eq. (3)], we can rewrite the impurity parallel momentum equation, Eq. (23), as

$$m_z n_z \frac{\partial}{\partial t}\delta u_{z,\|} + T_z\nabla_\|\delta n_z = -Zn_z\left(\nabla_\|\delta T_e + T_e\nabla_\|\frac{\delta n_e}{n_e}\right) + n_i m_i \nu_{iz}(\delta u_{i,\|} - \delta u_{z,\|}) \ . \qquad (25)$$

Substituting Eq. (21) into Eq. (25) to eliminate $\delta u_{i,\|}$, we obtain

$$\delta u_{z,\|} = -\frac{i}{\Omega_z}\cdot\nabla_\|\left\{c_{sz}^2\delta\hat{n}_z + \frac{m_i}{m_z}Zc_s^2\left[\delta\hat{n}_e + \delta\hat{T}_e + i\frac{n_i\nu_{iz}}{Zn_z\omega}(\delta\hat{n}_e(1+\tau_i) + \delta\hat{T}_e)\right]\right\} \ , \qquad (26)$$

where $\delta\hat{n}_e \equiv \delta n_e/n_e, \delta\hat{T}_e \equiv \delta T_e/T_e, \delta\hat{n}_z \equiv \delta n_z/n_z, c_{sz}^2 \equiv T_z/m_z$, and $\Omega_z \equiv \omega + i\nu_{iz}(1 + n_i m_i/n_z m_z)$. Combining Eqs. (22) and (26) determines $\delta\hat{n}_z$ in terms of $\delta\hat{\varphi}, \delta\hat{n}_e$, and $\delta\hat{T}_e$,

$$\delta\hat{n}_z = \frac{1}{1 - c_{sz}^2k_\|^2/\omega\Omega_z}\Bigg\{-\frac{\omega_{en}^*}{\omega}\left(\frac{L_n}{L_z}\right)\delta\hat{\varphi}$$

$$+\left(\frac{m_i}{m_z}Z\right)\frac{c_s^2k_\|^2}{\omega\Omega_z}\left[\delta\hat{n}_e + \delta\hat{T}_e + i\frac{n_i\nu_{iz}}{Zn_z\omega}(\delta\hat{n}_e(1+\tau_i) + \delta\hat{T}_e)\right]\Bigg\} \ , \qquad (27)$$

where $k_\| \equiv k_\|'x$ (we have transformed $\nabla_\| \to ik_\|$). For the dissipative drift wave the large impurity mass implies $c_{sz}^2k_\|^2 \ll \omega\Omega_z \sim \omega_{en}^{*2}$. Since $\delta\hat{\varphi}$, $\delta\hat{n}_e$, and $\delta\hat{T}_e$ are expected to be of the same order (verified a posterioi), and $L_n/L_z > 1$, the impurity density response can be asymptotically expressed in a simple form:

$$\delta\hat{n}_z \sim -\frac{\omega_{en}^*}{\omega}\frac{L_n}{L_z}\delta\hat{\varphi} \ . \qquad (28)$$

Notice that in the very low frequency case one can neglect ω in Ω_z. Futher, assuming that $1 \ll \nu_{iz}n_i m_i/n_z m_z$, and neglecting the second term of Eq. (27), one reproduces Rutherford's result[16,17] [$\kappa_z \equiv n_z T_z/m_i\nu_{iz}n_i$]

$$\delta\hat{n}_z = -\frac{\omega_{en}^*}{\omega + i\kappa_z k_\|^2}\cdot\frac{L_n}{L_z}\delta\hat{\varphi} \ , \qquad (29)$$

which can be a good approximation for the very low frequency rippling mode. For the current analysis, however, Eq. (28) is the proper approximation for the impurity response.

IV. The Eigenmode Equation, Numerical Results

In Sec. III, we discussed in detail the linearized dynamics of the neutral and impurity components. The appropriate ordering for the dissipative drift waves leads to the conclusion that the neutral density perturbations are negligibly, and that the impurity response is given by Eq. (28). The simplification was brought about by the fact that the perturbed impurity parallel velocity $u_{z,\|}$ is negligibly small for the mode under consideration. The smallness of $u_{z,\|}$ along with the neglect of the neutral response allows great simplification in the bulk plasma equations of motion which can then be readily solved. We do not consider ionization in this section ($\nu_I = 0$). All the simplified linearized equations are:

$$\omega\delta\hat{n} = \omega^*_{en}\delta\hat{\varphi} - k_\|(\delta\hat{J}_\| - \delta u_{i,\|}) \ , \tag{30}$$

where $\nu'_I \equiv T_e(\partial\nu_I/\partial T_e)$,

$$\delta\hat{J}_\| = (Z'\hat{J}_\|\Lambda_z - i\beta_\nu k_\|)\delta\hat{\varphi} + (Z'\hat{J}_\| + i\beta_\nu k_\|)\delta\hat{n} + (\frac{3}{2}\hat{J}_\| + i\beta_\nu k_\|)\delta\hat{T}_e \ , \tag{31}$$

with $Z' \equiv 1 - 1/Z_{\rm eff} \sim 1$, $\hat{J}_\| \equiv J_\|/en$, $\Lambda_z \equiv (\omega^*_{en}/\omega)(L_n/L_z)$, and $\delta\hat{J}_\| \equiv \delta J_\|/en$,

$$(\omega + \omega^*_{pi})\rho_s^2\nabla_\perp^2\delta\hat{\varphi} = -k_\|\delta\hat{J}_\| \ , \tag{32}$$

where $\rho_s \equiv c_s/\omega_{ci}$ with ω_{ci} the ion cyclotron frequency, and ω^*_{pi} is the ion diamagnetic frequency ($\equiv (1+\eta_i)\tau_i\omega^*_{en}$ with $\eta_i = dln\ T_i/dln\ n$),

$$(\omega + i\beta_\nu k_\|^2 + i\nu'_z)\delta\hat{T}_e = (\omega^*_{eT} + i\nu_z\Lambda_z)\delta\hat{\varphi} + k_\|(\delta u_{i,\|} - \delta\hat{J}_\|) \ , \tag{33}$$

where $\nu_z = (2/3)n_z I_z/T_e$, $\nu'_z = (2/3)n_z\partial I_z/\partial T_e$, and $\omega^*_{eT} = \eta_e\omega^*_{en}$ with $\eta_e \equiv dln\ T_e/dln\ n$, and

$$\delta u_{i,\|} = \frac{k_\| c_s^2}{\omega}\left[(1+\tau_i)\delta\hat{n} + \delta\hat{T}_e\right] \ . \tag{34}$$

Equations (30)-(34) are combined together to form the eigenmode equation,

$$\left(\frac{d^2}{d\overline{x}^2} - k^2\right)\delta\widehat{\varphi} + V(\overline{x})\delta\widehat{\varphi} = 0 \ , \tag{35}$$

where

$$V(\overline{x}) = \frac{1}{\widehat{\omega} + \widehat{\omega}_{pi}^*} \cdot \frac{P(\overline{x})}{Q(\overline{x})} \ , \tag{36}$$

$$P(\overline{x}) \equiv \overline{x}^2\Big\{\overline{x}^4\frac{1+\tau_i}{\widehat{\omega}} + \overline{x}^2\frac{L_s}{L_n}(1-\widehat{\omega}) - \overline{x}\frac{iZ'\Lambda_z\overline{J}_{\|}}{\overline{\beta}_\nu}\omega$$

$$+ \frac{i}{\overline{\beta}_\nu}\cdot\frac{L_s}{L_n}\cdot(\widehat{\omega}+i\widehat{\nu}_z')(\widehat{\omega}-1-\eta_e-i\widehat{\nu}_z\Lambda_z)\Big\} - \overline{x}\frac{Z'\Lambda_z\overline{J}_{\|}}{\overline{\beta}_\nu^2}\widehat{\omega}(\widehat{\omega}+i\widehat{\nu}_z') \ , \tag{37}$$

and

$$Q(\overline{x}) \equiv \overline{x}^4 - \overline{x}^2\frac{i}{\overline{\beta}_\nu}(3\widehat{\omega}+i\widehat{\nu}_z') - \frac{1}{\overline{\beta}_\nu^2}\widehat{\omega}(\widehat{\omega}+i\widehat{\nu}_z') \ . \tag{38}$$

In the eigenmode equation we retain the rippling effect due to impurity fluctuations only, namely, the $Z'\widehat{J}_{\|}\Lambda_z$ term, All frequencies (with a caret on top) are normalized to ω_{en}^*, for example, $\widehat{\omega} \equiv \omega/\omega_{en}^*, \widehat{\nu}_z \equiv \nu_z/\omega_{en}^*$. Other dimensionless quantities in Eq. (35)-Eq. (38) are $k \equiv \rho_s k_y(L_s/L_n)^{1/2}$, $x = \overline{x}\rho_s(L_s/L_n)^{1/2}$, $\overline{\beta}_\nu \equiv \beta_\nu k^2/L_s^2\omega_{en}^* = (m_i/m_e)(T_e c k_y/eBL_s)\cdot(1/Z_{\rm eff}\nu_{ei})$, and $\overline{J}_{\|} = (J_{\|}/enc_s)(L_s/L_n)^{1/2}$.

The eigenmode equation is clearly rather complicated and the potential $V(\overline{x})$ is a function of many parameters. Although some analytical solutions, which are quite good in the pertinent parameter range, will be presented in the next section, the major thrust of the current study is to numerically investigate the destabilizing effects of various competing mechanism, and to determine the nature of the wave function in regimes of interest.

We begin by displaying the numerically determined mode structure when the rippling effects, i.e., the contribution from the terms proportional to the equilibrium current $J_{\|}^{(0)}$ are neglected. For very small value of Υ [weakly collisional plasma, regime (a), $\Upsilon = 0.04$] a narrow current channel near the rational surface results in a very shallow potential well unable to contain the mode, which is primarily localized by the ion sound effect [Fig. 1*a*].

The situation illustrated in Fig. 1*b* is quite different. Here $\Upsilon = 0.18$ has a moderate value, and the current channel created potential value is deep enough to localize the mode; the ion sound term plays no essential role. As Υ is increased further [Fig. 1*c*, $\Upsilon = 0.6$] the current channel width increases towards $x = x_s$, and the structure of the mode becomes sensitive to the ion sound term. Finally, when $\Upsilon = 1$, the current channel, though broad, becomes sufficiently shallow that the mode structure is again controlled by the sound term [Fig. 1*d*]. Strictly speaking, our set of equations is inadequate to accurately describe the last scenario.

We now examine the comparative roles of the destabilizing mechanisms for standard edge plasma condition in TEXT. The parameters chosen for numerical work are: $R = 100cm$, $a = 25cm$, $n_e = 3 \times 10^{12} cm^{-3}$, $T_e = 20ev$, $B = 22kG$, $Z_{\text{eff}} = 3$, $L_n = 5cm$, $L_z = 1cm$, $L_s = 150cm$, $Z = 4$, V_{loop} (the loop voltage) $= 1Volt$, $\tau_i = 1.0$, $\eta_e = 1.0$, $\eta_i = 0.5$, and the poloidal mode number $m = 30$. [For the electron temperature $\sim$ 20ev, the impurity charge number is $Z \sim 4$]. From the given data, the impurity density can be calculated from the formula $n_z = (Z_{\text{eff}} - 1)n_e/16$. We do not include the effect from $\nu_z' (\sim \partial I_z/\partial T_e)$ for two reasons. First, the calculation based on the coronal model[19] indicates that the radiation cooling function $I_z(T_e)$ shows a strong dependence on T_e, and the charge state of impurities, so that the sign of ν_z' varies for different T_e's and charge states. On the other hand, the calculation based on the coronal model is subject to be modified due to transport in tokamak. An improved calculation including transport shows that the temperature dependence of I_z can be greatly decreased, accompanied by an enhancement in the magnitude of I_z.[20] In the light of the latter calculation, we choose $I_z(T_e) = 5.6 \times 10^{-19} \text{erg.cm}^{-3}/\text{s}$ as the standard value of the radiation cooling function, which corresponds to the peak value for carbon for $T_e \sim$ 10ev. All standard parameters are followed by the symbol (1), for example, the standard ν_{ei}, and ω_{en}^* are written as $\nu_{ei}(1) = 1.26 \times 10^6/\text{s}$, $\omega_{en}^*(1) = 2.18 \times 10^4/\text{s}$ respectively. From the above standard data, we obtain $\overline{\beta}_\nu(1) = 0.35$, $\hat{\nu}_z(1) = 0.2$, $k^2(1) = 0.04$, $\overline{J}_\parallel(1) = 0.1$.

By varying the value of the equilibrium current and collisionality, we can examine the

effects of 'rippling' on the mode structure, frequency, and growth rate. It is noticable that the 'rippling' becomes stronger as the plasma becomes more collisional. With stronger 'rippling' the mode localization is more skewed about the rational surface. This feature is shown in Fig. 2. Fig. 2*a* illustrates a dissipative drift wave slightly modified by the rippling effect, with its growth rate essentially determined by the impurity drive. Fig. 2*c* illustrates the case close to strong rippling regime; the instabilty in this case is mainly due to the rippling rather than the impurity drive. For different collisionalities we plot the mode frequencies and the growth rates versus the equilibrium current in Fig. 3. The standard value of the equilibrium current is indicated by an arrow in Fig. 3*b*, which suggests weak rippling. The condition for rippling to be important is that $Z'\widehat{J}_{||}\Lambda_z$ be not negligible compared to $\beta_\nu k_{||}$ [Eq. (31)]. This condition can be estimated as $Z'\overline{J}_{||}$ is bigger than about one third of $(L_z L_s/L_n^2)(\overline{\beta}_\nu/Z_{\text{eff}})^{1/2}$, when one has estimated the mode width by the current channel width, and the mode frequency by ω_{en}^*.

The real frequencies and growth rates normalized to the standard diamagnetic frequency $\omega_{en}^*(1)$ versus the poloidal mode number m (and the corresponding k_y) are shown in Fig. 4 for various L_z with other parameters taken at the standard values. It shows that the peak of growth rate shifts towards higher m for greater growth rate. The marginal stability curves are shown for standard values in parameter spaces [$L_z - L_n$ plane in Fig. 5, and $L_z - T_e$ plane in Fig. 6]. These curves indicate that the lower electron temperature and smaller density gradient favor instability for fixed impurity gradient. For lower electron temperature the parallel heat conduction is smaller, resulting in a smaller damping rate. For smaller density gradients, although the shear damping becomes larger, the increase in the impurity drive overtakes the damping increase, and the mode actually tends to be more unstable.

Several analytical expressions for the dispersion relation are given in the next section, where the general features of the instability are shown. For example, η_e is stabilizing to the dissipative drift wave.

V. Analytical Solutions

The main thrust of this paper is to numerically investigate the dissipative drift instability in the tokamak edge plasmas. However, in the regime of greatest interest (from the experimental point of view), i.e., when the parameter Υ is not too small but still less than unity [regime (b)], we have been able to derive an analytical dispersion relation which agrees very well with the numerical work, and which clearly brings out the parameter dependence of the growth rate.

From numerical work presented in Sec. IV, we concluded that in the regime of moderately high collisionality, the effects of both the sound and the rippling (due to the equilibrium current) terms is negligible. The modes turn out to be localized in distances smaller than the sound turning point. For these modes, the relevant equation, an approximate version of Eq. (35), can be written as $[\tau_i = 0, k = 0]$,

$$\frac{d^2}{d\overline{x}^2}\delta\widehat{\varphi} + \frac{1}{\widehat{\omega}} \cdot \frac{P(\overline{x})}{Q(\overline{x})}\delta\widehat{\varphi} = 0 \ , \tag{39}$$

with

$$\frac{P(\overline{x})}{Q(\overline{x})} \sim -\overline{x}^2 \frac{a_1\overline{x}^2 + a_0}{b_1\overline{x}^2 + b_0} \ , \tag{40}$$

where

$$a_1 = \frac{L_s}{L_n}(1 - \widehat{\omega}) \ , \tag{41}$$

$$a_0 = -i\frac{\widehat{\omega}}{\overline{\beta}_\nu} \cdot \frac{L_s}{L_n}\left(1 + \eta_e - \widehat{\omega} + i\frac{\widehat{\nu}_z\Lambda_z}{\widehat{\omega}}\right) \equiv -i\frac{\widehat{\omega}}{\overline{\beta}_\nu} \cdot \frac{L_s}{L_n} f(\widehat{\omega}) \ , \tag{42}$$

$$b_1 = \frac{i}{\overline{\beta}_\nu}(3\widehat{\omega} - i\widehat{\nu}_z) \ , \tag{43}$$

$$b_0 = \left(\frac{\widehat{\omega}}{\overline{\beta}_\nu}\right)^2 \ , \tag{44}$$

and $\widehat{\omega} \equiv (\widehat{\omega} + \widehat{\omega}^*_{pi})$. Notice that for edge plasmas L_s/L_n is a large number, and for the moderately collisional plasmas under investigation, $\widehat{\omega}/\overline{\beta}_\nu \gg 1$. In a formal ordering one

could take $L_s/L_n \sim 1/\epsilon \sim \widehat{\omega}/\overline{\beta}_\nu$, ϵ being the small ordering parameter. For the modes with spatial extent limited to $\overline{x}^2 < 1/\epsilon$, Eq. (39) is a good approximation to Eq. (35).

The zeros of $P(\overline{x})$ in the complex plane determine the turning points of the system, $\overline{x} = 0, \overline{x} = \pm(-a_0/a_1)^{1/2} \equiv \pm x_t$. A W.K.B. dispersion relation corresponding to the principle mode confined between $-x_t$ and x_t is

$$\frac{\pi}{2} = \left(\frac{1}{\widehat{\omega}}\right)^{1/2} 2\int_0^{x_t} d\overline{x}\overline{x} \left(\frac{a_1\overline{x}^2 + a_0}{b_1\overline{x}^2 + b_0}\right)^{1/2} , \tag{45}$$

which is readily evaluated to yield

$$\frac{\pi}{2} = \left(\frac{a_1}{b_1\widehat{\omega}}\right)^{1/2} \left(\frac{b_0}{b_1} - \frac{a_0}{a_1}\right)^{1/2} \left[\sin^{-1}\Pi - \Pi(1-\Pi^2)^{1/2}\right] , \tag{46}$$

where $\Pi = (1 - a_1b_0/a_0b_1)^{-1/2}$. Several such transcendental dispersion relation can be obtained by including k^2 and/or the sound term. However, their utility in producing insights or suggesting scaling of the growth rate becomes questionable as their complexity increases. In fact, the dispersion relation given by Eq. (46) is also not particularly perspicous. Considerable simplifications result if we use the perfectly valid ordering (for the range of interest) $b_0/b_1 \gg 1$ along with $|b_0/b_1| > |a_0/a_1|$, which is satisfied only if the dispersion relation corresponds to $f(\widehat{\omega}) \sim 0$. This indeed happens to be the case and Eq. (46), then, reduces to

$$a_0\left(-\frac{a_0}{b_0\widehat{\omega}}\right)^{1/2} = -\frac{3\pi}{4}\left(a_1 - \frac{b_1a_0}{2b_0}\right) \sim -\frac{3\pi}{4}a_1 , \tag{47}$$

which can be reexpressed in terms of physical variables.

$$f(\widehat{\omega}) \equiv 1 + \eta_e - \widehat{\omega} - i\frac{\widehat{\nu}_z\Lambda_z}{\widehat{\omega}} = e^{i\pi/6}\left(\frac{3\pi}{4}\right)^{2/3}\left(\overline{\beta}_\nu\frac{L_n}{L_s}\right)^{1/3}\left(1 + \frac{\widehat{\omega}^*_{pi}}{\widehat{\omega}}\right)^{1/3}(1+\widehat{\omega})^{2/3} . \tag{48}$$

Mode frequencies, determined from Eq. (48), over a broad range of $L_n/L_s, \overline{\beta}_\nu$, and η_e agree very well with the results of the direct numerical integration of Eq. (35). Whenever the impurity drive ($\sim \nu_z\Lambda_z$) is strong enough, i.e., the situation of interest for the present study, even the grossly simple dispersion relation $f(\widehat{\omega}) = 0$ yields essentially correct growth rates as

well as the oscillation frequencies. Dispersion relation similar to Eq. (48) have been derived by Drake and Hassam.[13] These, rather, simple straightforward expressions for the linear growth rate can be extremely useful in understanding the quasi - linear and nonlinear stage of the mode. For example, we consider a quasi-linear saturation of the mode, achieved by the relaxation of the impurity gradient due to the enhanced fluctuation amplitude. Following the standard approach of the quasi-linear calculation, wherein Eq. (48) is used for the linear dispersion, we obtain the scaling for the saturated mode amplitude $\delta\widehat{\varphi} \sim \widehat{\nu}_z(L_s/L_n\overline{\beta}_\nu)^{1/3}$, where $\widehat{\nu}_z$ stands for the contribution from the driving force, whereas $(L_s/L_n\overline{\beta}_\nu)^{1/3}$ stands for the damping rate. This scaling implies that the fluctuation level is proportional to the impurity density.

VI. Effects of Ionization

Since ionization is a universal characteristics of the edge plasmas, an instability driven by ionization could be an extremely attractive possibility for understanding and explaining the ever existence of large levels of fluctuations in edge plasmas. However, consistent inclusion of ionization into the mode equation turns out to be a tricky proposition. In this section we point out the difficulty through a variety of examples. We limit ourselves only to a conventional linear analysis; the fluctuations are taken to be infinitely small, so that any slow spatial and temporal variation of physical quantities arising from the ensemble average of fluctuations can be neglected with respect to the variation in the quiescent plasma.

It is expected that the leading effect of ionization on the mode stability will come from the source term in the continuity equation. In the absence of fluctuations, the electron continuity equation takes the form $[n_e = n_e^{(0)} + \delta n_e, \mathbf{v}_e = \mathbf{v}_e^{(0)} + \delta\mathbf{v}_e]$

$$\frac{\partial n_e^{(0)}}{\partial t} + \nabla\cdot(n_e^{(0)}\mathbf{v}_e^{(0)}) = \nu_I^{(0)} n_e^{(0)} \ , \tag{49}$$

where for a genuine equilibrium $\partial n_e^{(0)}/\partial t = 0$. We pointed out earlier (Sec. II) that in a

linear slab model with gradients only along x the divergence of the electron flow vanishes implying that there is no equilibrium electron density as long as $\nu_I^{(0)} \neq 0$. This may easily be the case in early stages of the tokamak discharge. In this case, since the 'equilibrium' density varies at precisely the rate ($\nu_I^{(0)}$) at which one seeks an ionization driven instability, this time variation has to be properly considered in the stability analysis; the solution of the initial value problem becomes nontrivial, and a naive Fourier analysis in time could result in serious errors. In principle, one could solve this problem using two time scale perturbation theory if $\nu_I^{(0)} \ll \omega$. This procedure is rather complicated, and is being investigated.

In order to demonstrate the surprises associated with ionization, we analyze a 'toy' problem of collisionless drift waves neglecting the effects of impurities of charge exchange, and of $\delta\nu_I$, τ_i (the finite ion temperature), and δT_e. The pertinent linear problem (spatial Fourier transform in y and z have been taken) consists of the following set:

$$i\frac{\partial}{\partial t}\delta\hat{n} = \omega_{en}^{*}(t)\delta\hat{\varphi} - k_{\|}\delta\hat{J}_{\|} + k_{\|}\delta u_{i,\|} \ , \tag{50}$$

$$\delta\hat{n} = \delta\hat{\varphi} \ , \tag{51}$$

$$i\frac{\partial}{\partial t}\rho_s^2\nabla_{\perp}^2\delta\hat{\varphi} = -k_{\|}\delta\hat{J}_{\|} \ , \tag{52}$$

$$i\frac{\partial}{\partial t}\delta u_{i,\|} = k_{\|}c_s^2\delta\hat{n} \ , \tag{53}$$

where $\delta\hat{n} \equiv \delta n/n^{(0)}(t), \delta\hat{J}_{\|} \equiv \delta J_{\|}/en^{(0)}(t)$. With this choice of variables, the only explicit time dependence comes through $\omega_{en}^{*}(t) \equiv -(T_e^{(0)}ck_y/eB)(\partial/\partial x)ln\ n^{(0)}(t)$. From Eq. (12) we know that [N^0 = constant in time]

$$n^{(0)}(t) = N^0(x)\exp\left[\int dt\nu_I^{(0)}(x,t)\right] \ , \tag{54}$$

where

$$\frac{\partial}{\partial x}ln\ n^{(0)}(t) = \frac{1}{N^{(0)}}\exp\left[-\int dt\nu_I^{(0)}\right]\frac{\partial}{\partial x}N^{(0)}(x)\exp\left[+\int dt\nu_I^{(0)}\right] \ , \tag{55}$$

leading to the conclusion that if $\nu_I^{(0)}(x,t)$, the ionization rate, were independent of x, the entire set would have no explicit time dependence in the coefficients multiplying the perturbed

quantities. Thus the eigenvalue problem will be amenable to the usual Fourier treatment with the astonishing result that the ionization has completely disappeared from the eigen equation! The perturbed density still increases due to ionization, but it, by no means, can be viewed as an instability driven by ionization, because other fluctuating quantities (the electrostatic field, for example) see no effects due to ionization. In this 'toy' problem, ionization effects (not trivially calculable) persist only if $\nu_I^{(0)}$ or equivalently the neutral density has spatial gradients.

To continue our analysis of this problem, we now consider two cases, where a genuine equilibrium density has been achieved. It may happen if we include the electron radial velocity, that has been neglected in Eq. (2). The Braginskii model, then, yields

$$v_{e,x} = -D_x \left[(1+\tau_i) \frac{d}{dx} ln\ n + \frac{1}{T_e} \frac{dT_i}{dx} - \frac{1}{2} \frac{d}{dx} ln\ T_e \right] , \tag{56}$$

where $D_x \equiv (1/2)\rho_e^2 \nu_{ei} > 0$ with ρ_e the electron Larmor radius.[11,21] Substituting Eq. (56) into the eqilibrium electron continuity equation, we find that

$$\left[\frac{d}{dx} + \left(\frac{d}{dx} ln\ n^{(0)} \right) \right] D_x^{(0)} \left[(1+\tau_i^{(0)}) \frac{d}{dx} ln\ n^{(0)} + \frac{1}{T_e^{(0)}} \frac{dT_i^{(0)}}{dx} - \frac{1}{2} \frac{d}{dx} ln\ T_e^{(0)} \right] + \nu_I^{(0)} = 0 , \tag{57}$$

must be satisfied. Since $D_x^{(0)}$ is very small, one must have very steep profiles to balance the finite $\nu_I^{(0)}$. Sharp gradients make it imperative that the radial component of $\delta \mathbf{v}_e$ be retained in the linearized electron continuity equation [Eq. (13)]. Making use of the linearized form of Eq. (56), we can evaluate the contribution from the radial flow to $\nabla \cdot \delta \mathbf{v}_e + \delta \mathbf{v}_e \cdot \nabla ln\ n_e^{(0)}$ [needed in Eq. (13)],

$$\frac{d}{dx} \delta v_{e,x} + \delta v_{e,x} \frac{d}{dx} ln\ n^{(0)} = -\frac{\delta n}{n^{(0)}} \left[\frac{d}{dx} + \left(\frac{d}{dx} ln\ n^{(0)} \right) \right]$$

$$\cdot D_x^{(0)} \left[(1+\tau_i^{(0)}) \frac{d}{dx} ln\ n^{(0)} + \frac{1}{T_e^{(0)}} \frac{dT_i^{(0)}}{dx} - \frac{1}{2} \frac{d}{dx} ln\ T_e^{(0)} \right] + \ldots = \nu_I^{(0)} \frac{\delta n}{n^{(0)}} + \ldots , \tag{58}$$

where '...' consists of terms proportional to $(d/dx)(\delta n/n^{(0)}), (d^2/dx^2)(\delta n/n^{(0)}), \delta T_e/T_e^{(0)}$ etc., and Eq. (57) has been used to simplify the second equation. Substituting Eq. (58) into

Eq. (13), we obtain

$$\left(\frac{\partial}{\partial t}+\mathbf{u}_E^{(0)}\cdot\nabla+\nu_I^{(0)}+\ldots\frac{d}{dx}+\ldots\frac{d^2}{dx^2}\right)\frac{\delta n}{n^{(0)}}=\ldots\delta\widehat{\varphi}+\ldots\delta\widehat{T}_e\ . \tag{59}$$

Obviously, the $\nu_I^{(0)}$ term in Eq. (59), now seems to have a stabilizing effect, although the total effect due to the equilibrium is rather complicated. Thus, a consistent understanding of the equilibrium seems to have converted ionization into a stabilizing force, though naively one could have judged it to be destabilizing. Equation (57) does not correspond to a realistic tokamak plasma even if $D_x^{(0)}$ is enhanced by the Pfirsch-Schluter effect.[22] This example is given just for illustration.

There exists an alternative mechanism that may also result in an equilibrium. Let us consider a poloidally localized ionization source, which can be modeled by $\nu_I[H(y)-H(y-y_0)]$ where $H(y)$ is the Heaviside step function, and $a/m \ll y_0 \ll a$ (a is the minor radius and m is the poloidal mode number). An equilibrium in the ionization region can be achieved by a finite density gradient in the poloidal y-direction, i.e., the continuity equation reduces to

$$\frac{c}{B}\frac{d\varphi^{(0)}}{dx}\cdot\frac{d}{dy}ln\ n^{(0)}=\nu_I^{(0)}\ . \tag{60}$$

which can be readily satisfied. Such an equilibrium requires a modified slab model; the density $n^{(0)}$ may vary in y-direction, while other equilibrium quantities such as $\varphi^{(0)}$, $T_e^{(0)}$ vary only in the radial x-direction. The finite density gradient in y will add extra terms to our basic system. For example, $\omega_{en}^{*}\delta\widehat{\varphi}$ in Eq. (30) will be modified to

$$\left(\omega_{en}^{*}+i\frac{T_e^{(0)}\nu_I^{(0)}}{eE_x^{(0)}}\cdot\frac{d}{dx}\right)\delta\widehat{\varphi}\ , \tag{61}$$

where $E_x^{(0)}\equiv -d\varphi^{(0)}/dx$. For the dissipative drift wave $\Delta x\sim\rho_s(L_s/L_n)^{1/2}$, and the new term ($\sim\nu_I^{(0)}$) can be important for the parameters relevant to TEXT. However, it is not easy to estimate the effect of $\nu_I^{(0)}$ on the instability until the entire system is analyzed. The equilibrium described by Eq. (60) may be a possible choice. For many experiments performed

in TEXT the neutral source is indeed highly localized in poloidal direction. However, this may not be the experimentally observed equilibrium, at least, in the flat plasma current phase. It is possible that the observed equilibrium may be a nonlinear equilibrium in which the electron radial flow (the radial particle diffusion) due to nonlinear (turbulent) transport may be large enough to balance the ionization source, so that the density gradient in y becomes small, even ignorable. This is beyond the scope of conventional linear analysis, to which this paper is limited.

All three examples discussed in the section clearly illustrate that a knowledge of the mechanism leading to an equilibrium (genuine and not genuine) is essential for a correct evaluation of the role of ionization in determining mode stability. The general problem is quite complicated, and the results depend upon the nature of the equilibrium. It is clear that the direct measurements on the equilibrium, and on the electron radial flow at various poloidal positions and different discharge phases will be crucial in understanding the role of ionization in tokamak dynamics. This subject will be dealt with in a forthcoming publication.

VII. Summary and Conclusions

We have examined the linear stability of the electrostatic dissipative drift wave for conditions pertinent to tokamak edge plasmas. There are two principal conclusions of this study. First of all, we find that when properly evaluated, the impurity condensation associated with radiation cooling can serve as an important destabilizing mechanism provided the impurity density gradients are sharper than the density gradients of the plasma. For standard parameters the growth rate can be a reasonable fraction of the diamagnetic drift frequency. Detailed comparison with TEXT experiments requires more information on impurity profiles, and will be presented elsewhere. However, we note that this driving mechanism may be interesting to the understanding of two types of (ELM dominated and ELM free) H-modes in ASDEX, which appear to be associated with different impurity profiles.[23–25]

Our second result concerns the effects of ionization. We find that these effects are completely determined by the processes which lead to an 'equilibrium' in the presence of a steady source of particles. By analyzing a few possible scenarios, we showed that it is difficult to make a clear case that ionization drives drift waves unstable; the real problem is rather complicated. Thus, any naive notions concerning a direct ionization drive for the plasma edge modes need critical and careful scrutiny.

Acknowledgments

The authors wish to acknowledge stimulating discussions with Ch.P. Ritz, D. Ross, A. Wootton, B. Rowan, P. Valanju, and E. Solano. The work is supported by the U.S. Department of Energy contracts #DEFG05-80ET-53088 and #DEFG05-80ER-53266.

References

1. R.J. Thayer and P.H. Diamond, Phys. Rev. Lett. **65**, 2784 (1990).

2. ASDEX TEAM, Nucl. Fusion **29**, 1959 (1989).

3. R.D. Stambaugh, S.M. Wolfe, R.D. Hawryluk, J.H. Harris, H. Biglari, S.C. Prager, R.J. Goldston, R.J. Fonck, T. Ohkawa, B.G. Logan, and E. Oktay, Phys. Fluids B **2**, 2941 (1990).

4. K.H. Burrel, T.N. Carlstron, E.J. Doyle, P. Gohil, R.J. Groebner, T. Lehecka, N.C. Luhmann, H. Matsumoto, T.H. Osborne, W.A. Peebles, and R. Philipona, Phys. Fluids B **2**, 1405 (1990).

5. R.J. Taylor, M.L. Brown, B.D. Fried, H. Grote, J.R. Liberati, G.J. Morales, and P. Pribyl , Phys. Rev. Lett. **63**, 2365 (1989).

6. R.J. Groebner, K.H. Burrel, and R.P. Seraydarian, Phys. Rev. Lett. **64**, 3015 (1990).

7. Ch.P. Ritz, H. Lin, T.L. Rhodes, and A. Wootton, Phys. Rev. Lett. **65**, 2543 (1990).

8. L. Garcia, P.H. Diamond, B.A. Carreras, and J.D. Callen, Phys. Fluids **28**,2147 (1985).

9. D.R. Thayer and P.H. Diamond, Phys. Fluids **30**, 3724 (1987).

10. H. Lin, Roger D. Bengtson, and Ch.P. Ritz, Phys. Fluids B **1**, 2027 (1989).

11. S.I. Braginskii, in *Review of Plasma Physics*, ed. M.A. Leotovich (Consultants Bureau, New York 1965), Vol. 1, p. 205.

12. B.D. Scott, Phys. Rev. Lett. **65**, (1990).

13. J.F. Drake and A.B. Hassam, Phys. Fluids **24**, 1262 (1981).

14. A.B. Hassam and J. F. Drake, Phys. Fluids **26**, 133 (1983).

15. L. Chen, P.N. Guzdar, J.Y. Hsu, P.K. Kaw, C. Oberman, and R. White, Nucl. Fusion **19**, 373 (1979).

16. R.H. Rutherford, in *Physics of Plasma Close to Thermonuclear Conditions*, ed. B. Coppi (Pergamon, New York, 1981), Vol. I, p. 143.

17. T.S. Hahm, P.H. Diamond, P.W. Terry, L. Garcia, and B.A. Carreras, Phys. Fluids. **30**, 1452 (1987).

18. J.F. Drake, Phys. Fluids **19**, 2429 (1987).

19. D.E. Post, R.V. Jensen, C.B. Tarter, W.H. Grasberger, and W.A. Lokke, in *Report of Princton Plasma Physics Laboratory* PPPL-1352, July 1977.

20. B. Rowan, Private communications.

21. F.L. Hinton and R.D. Hazeltine, Rev. Mod. Phys. **48**, 239 (1976).

22. D. Pfirsch and A. Schlueter, Max Planck Institute Report MPI/PA/7/62(1962).

23. M. Keilhacker *et al.*, in *Plasma Physics and Controlled Nuclear Fusion Research 1984*, London (IAEA, Vienna, 1985), Vol. I, p. 71.

24. O. Gruber *et al.*, in *Proceedings of the Twelfth European Conference on Controlled Fusion and Plasma Physics*, Budapest (EPS, Petit - Lancy, Switherland, 1985), Part I, p. 18.

25. R. Mueller, G. Janeschitz, P. Smeulders, and Fussmann, Nucl. Fusion **27**, 1817 (1987).

Figure Captions

1. The structure of the eigenmode and potential well for different regimes. Figures (a) to (d) are for $\Upsilon = 0.04,\ 0.18,\ 0.6$, and 1.0 respectively. The solid curves and dashed curves stand for real and imaginary part. The bold lines represent the potential well. The thin lines represent the eigenmode. The horizontal axis is normalized to the ion sound width x_s.

2. The eigenmode structure with rippling effects at $Z'\overline{J}_{||} = 0.5$. Figures (a) to (c) are for $\overline{\beta}_\nu = 0.5,\ 0.35$, and 0.1 respectively. Other parameters are standard parameter.

3. The real frequencies (a) and growth rates (b) versus $Z'\overline{J}_{||}$ for $\overline{\beta}_\nu = 0.5, 0.35$, and 0.1. The corresponding curves are denoted by a, b, and c respectively. Other parameters are standard parameters. The arrow in (b) indicates the standard value of $Z'\overline{J}_{||}$.

4. The real frequencies and growth rates in terms of the standard value $\omega^*_{en} = 2.18 \times 10^4/s$ versus the poloidal number m for $L_z = 2.0cm,\ 1.5cm,\ 1.0cm$, and $0.5cm$. The corresponding curves are denoted by a, b, c, and d respectively. Other parameters are standard parameters.

5. The marginal stability curves for different plasma densities in the $L_n - L_z$ plane. The curve a, b, and c stand for the density $n_e = 3,\ 6,\ 9 \times 10^{12} cm^{-3}$ respectively. Other parameters are standard parameters. Below the curve is the unstable region.

6. The marginal stability curves for different L_n in the $T_e - L_z$ plane. The curve a, b stand for $L_n = 2cm$, and 5cm respectively. Other parameters are standard parameters. Below the curve is the unstable region.

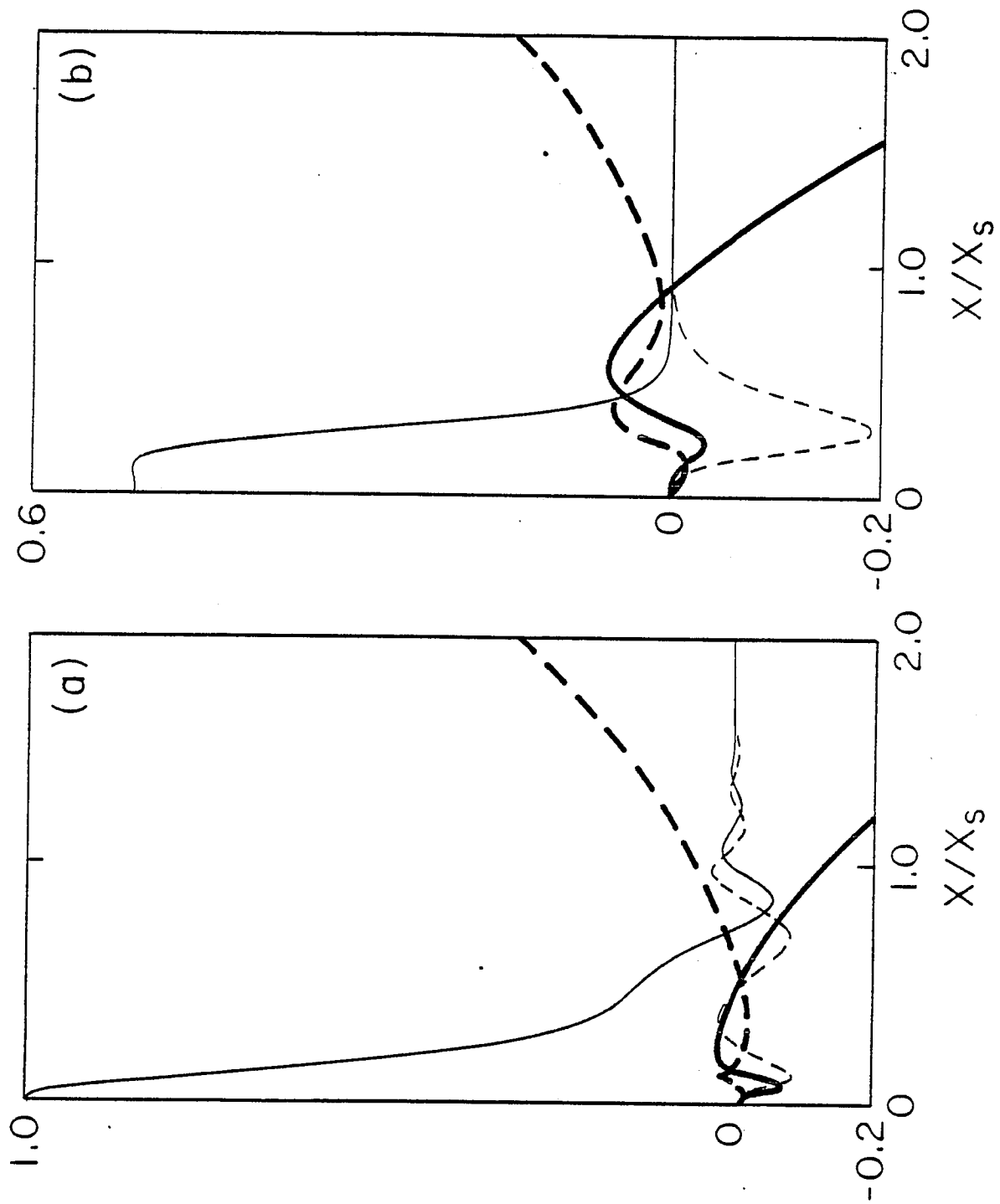

Fig. 1

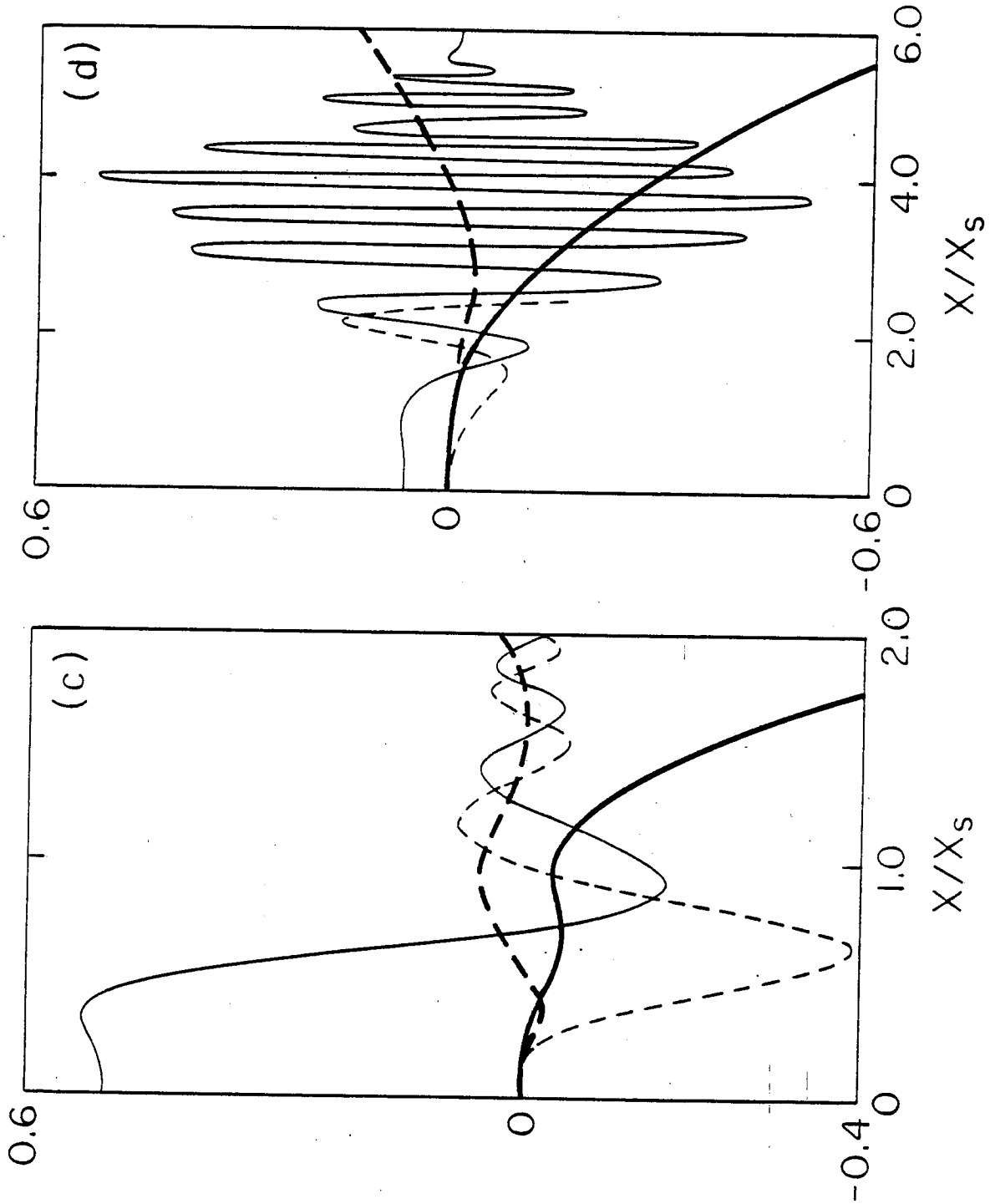

Fig. 1 (cont'd)

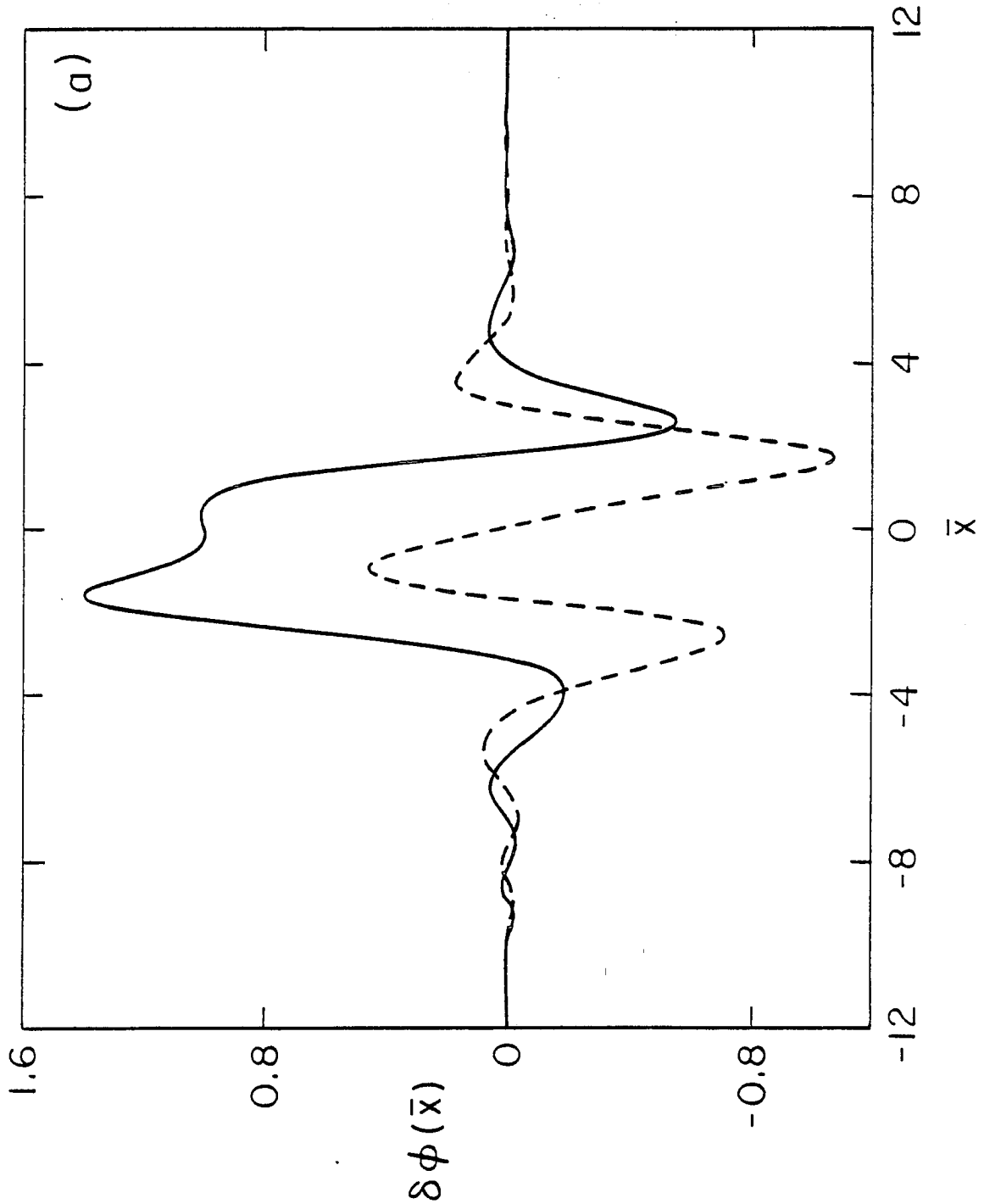

Fig. 2

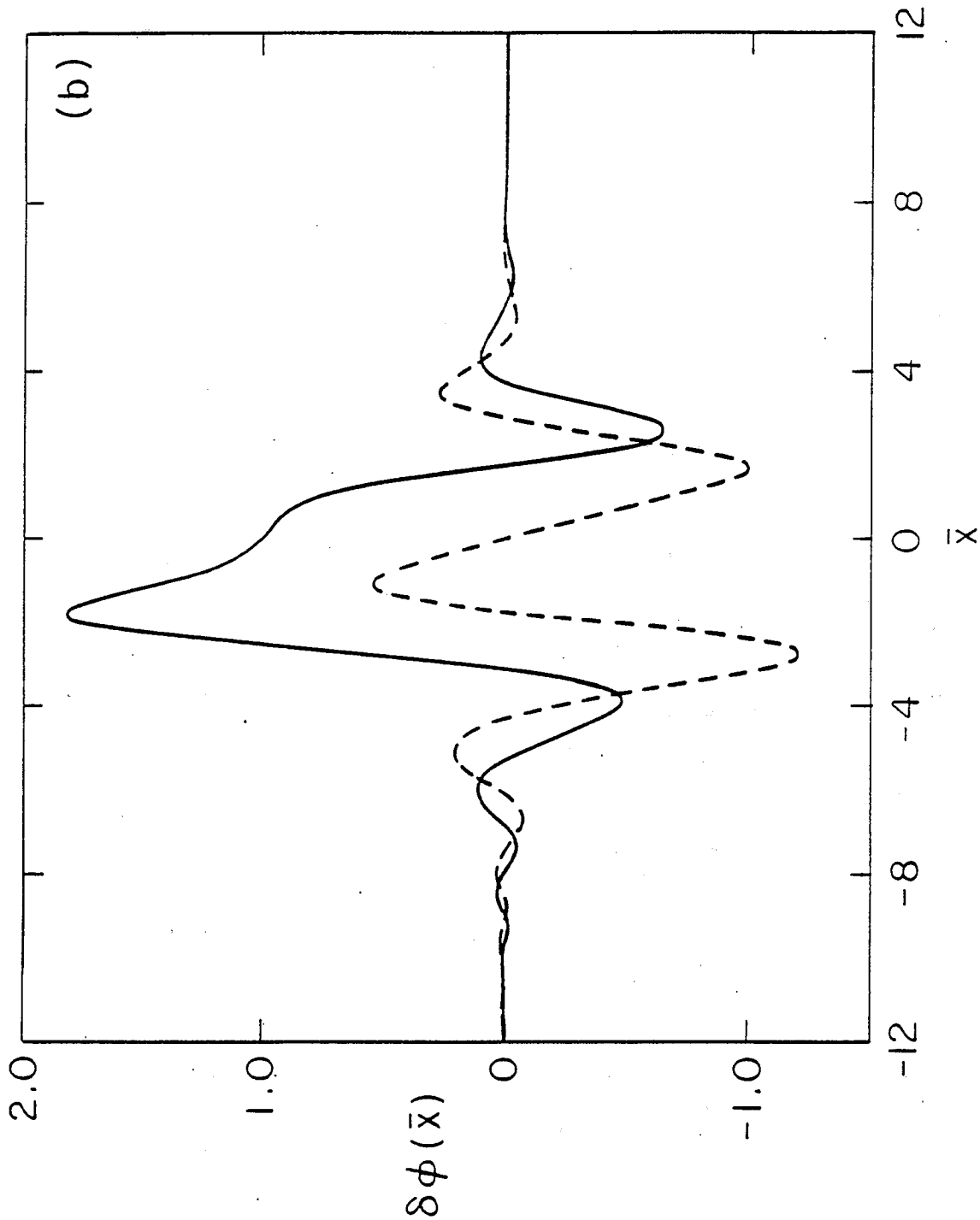

Fig. 2 (cont'd)

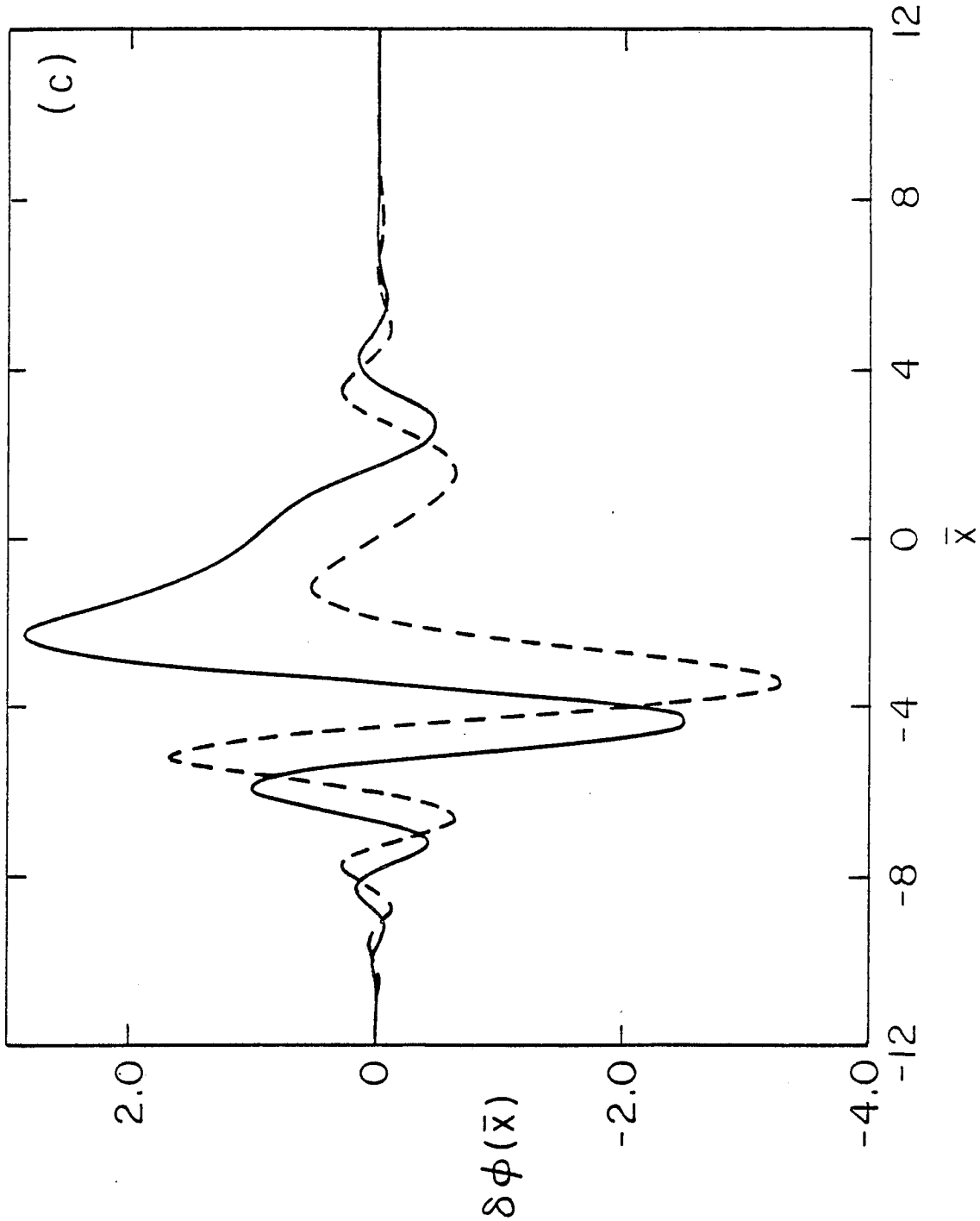

Fig. 2 (cont'd)

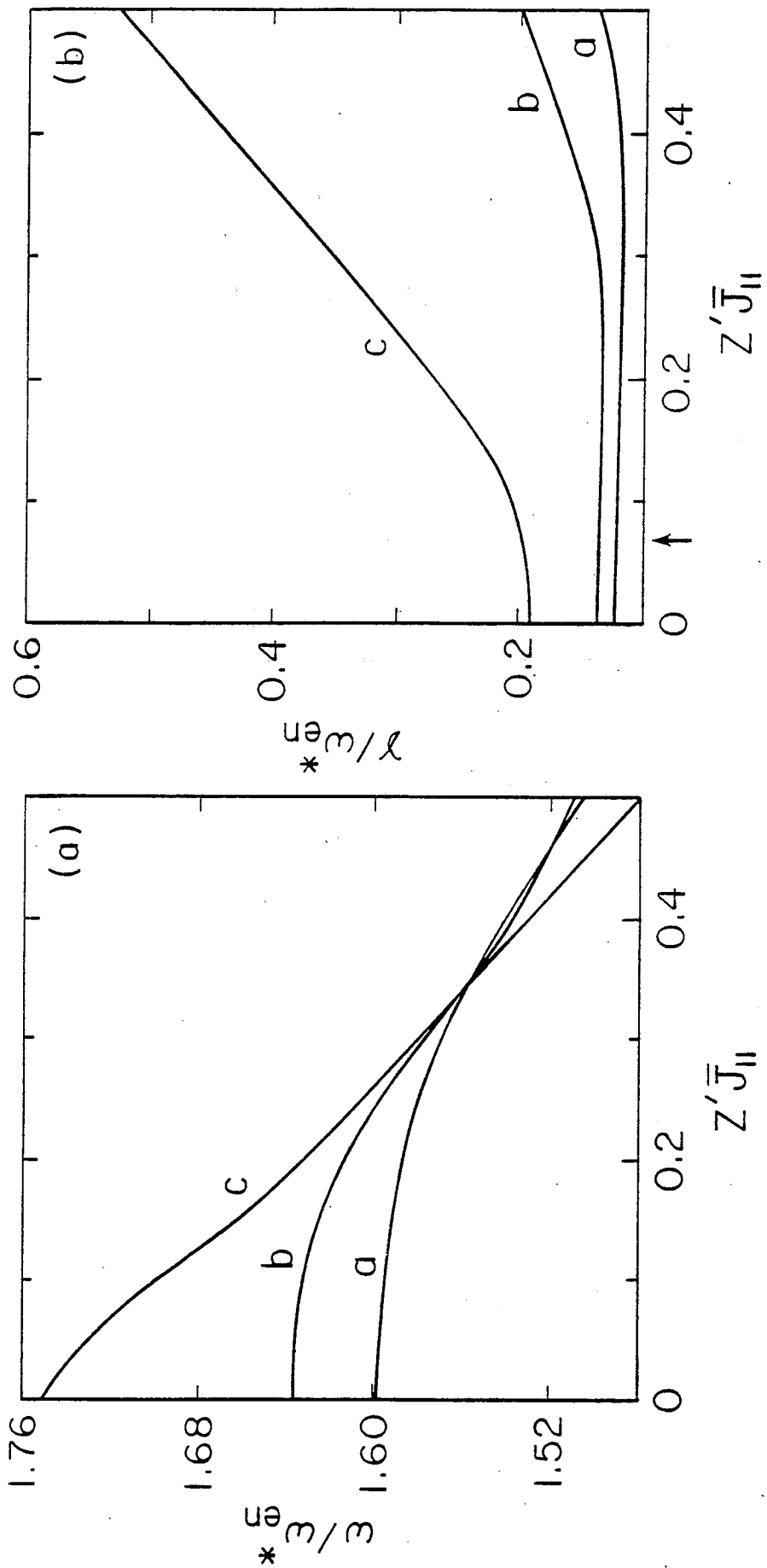
(b)
a
b
c
0.6
0.4
0.2
0
0.2
0.4
γ/ω_{en}^*
$Z'\bar{J}_{11}$
(a)
a
b
c
1.76
1.68
1.60
1.52
0
0.2
0.4
ω/ω_{en}^*
$Z'\bar{J}_{11}$

Fig. 3

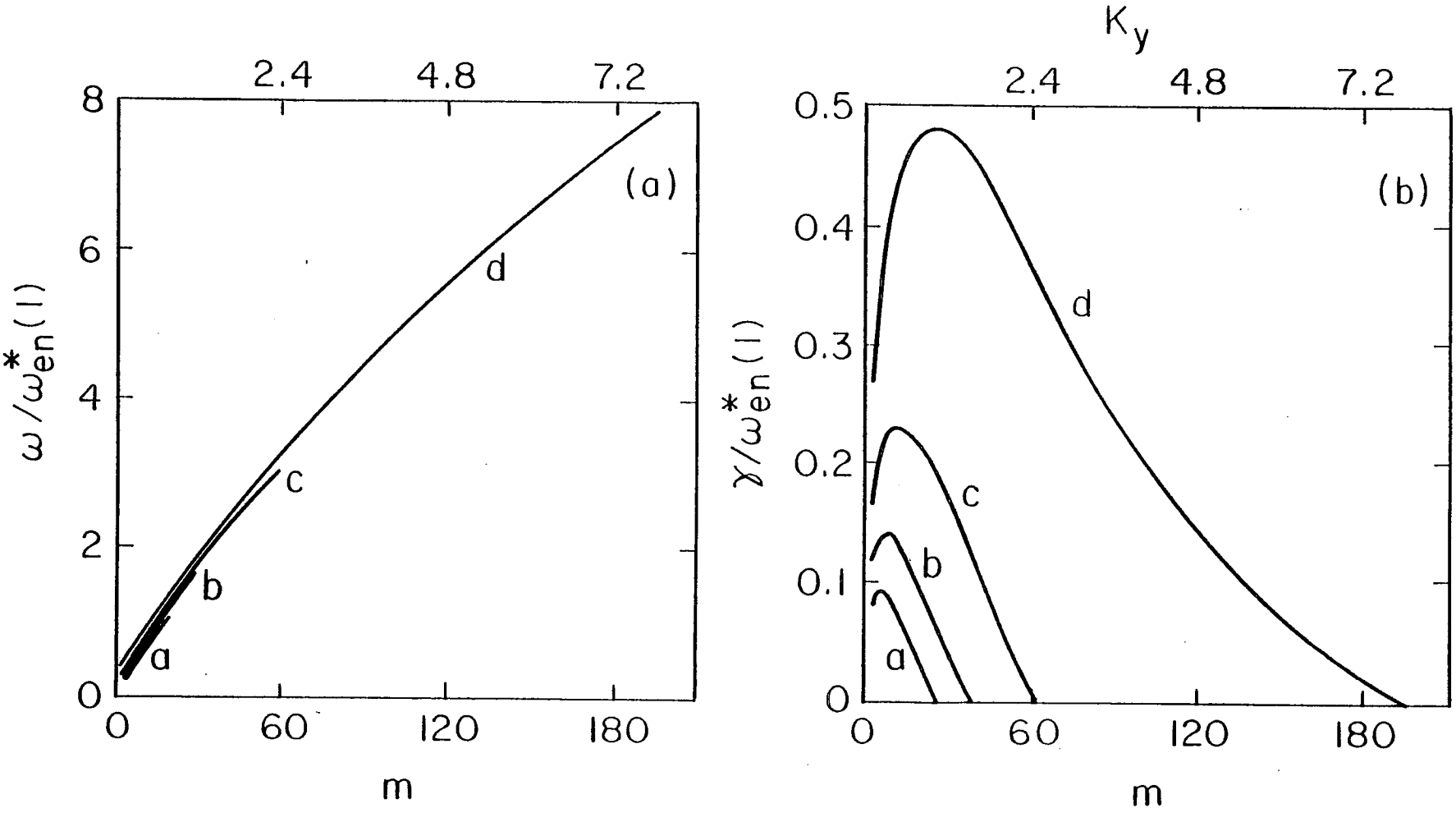
2.4
4.8
7.2
8
6
4
2
0
$\omega/\omega^*_{en}(1)$
(a)
d
c
b
a
0
60
120
180
m
K_y
2.4
4.8
7.2
0.5
0.4
0.3
0.2
0.1
0
$\gamma/\omega^*_{en}(1)$
(b)
d
c
b
a
0
60
120
180
m

Fig. 4

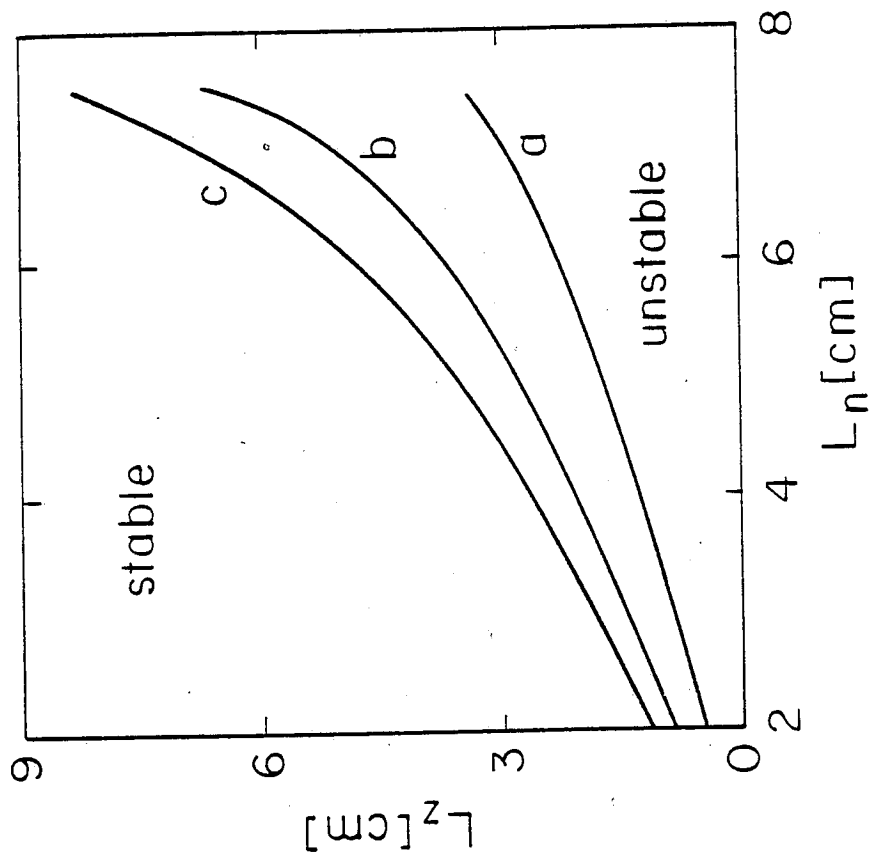

Fig. 5

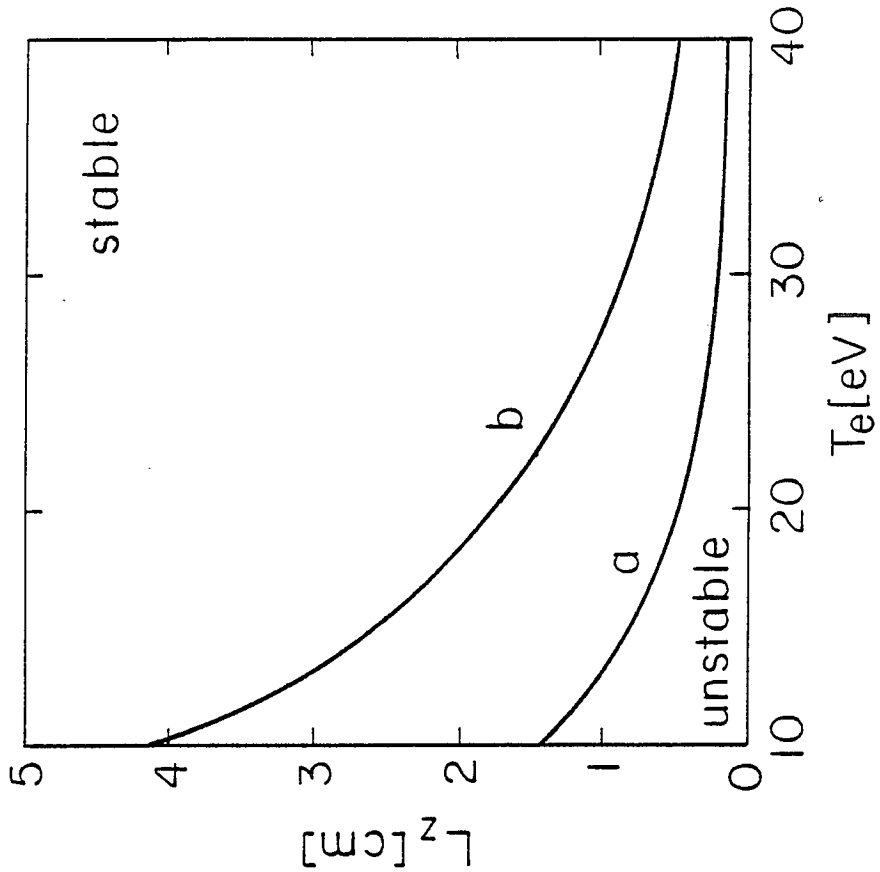

Fig. 6